

THE CRYSTAL STRUCTURE OF
NARSARSUKITE, $\text{Na}_2\text{TlOSi}_4\text{O}_{10}$

by

DONALD RALPH PEACOR
S.B., TUFTS UNIVERSITY
(1958)



SUBMITTED IN PARTIAL FULFILLMENT
OF THE REQUIREMENTS FOR THE
DEGREE OF MASTER OF
SCIENCE
at the
MASSACHUSETTS INSTITUTE OF
TECHNOLOGY
June, 1960

Signature of Author

Department of Geology, May 15, 1960

Certified by

11/1/60 Thesis Supervisor

Accepted by .

Chairman, Departmental Committee
on Graduate Students

The Crystal Structure of Narsarsukite, $\text{Na}_2\text{TlOSi}_4\text{O}_{10}$

Donald R. Peacor

Submitted to the Department of Geology on May 21, 1960

in partial fulfillment of the requirements for the
degree of Master of Science.

Abstract

The space group of narsarsukite has been confirmed to be $I4/m$. The unit cell dimensions are $a = 10.7260 \pm .0002 \text{ \AA}$ and $c = 7.948 \pm .001 \text{ \AA}$, and the unit cell contains 4 $\text{Na}_2\text{TlOSi}_4\text{O}_{10}$. Three-dimensional intensity data were obtained with the single-crystal Geiger-counter diffractometer. After correcting for Lorentz and polarization factors and absorption, the intensity data were used to compute a full three-dimensional Patterson synthesis. Restrictions placed on the location of titanium atoms by equipoint ranks enabled a complete set of minimum-function maps based on titanium images to be constructed. Despite ambiguities, these maps, in conjunction with interpretations of the implication diagram $I4(xy0)$ and the Harker line $[00z]$, provided the locations of the silicon and titanium atoms. The silicon inversion peak on the Patterson maps was then located, and a complete set of minimum-function maps based on the silicon inversion peak was constructed. All atoms were located on these maps with no ambiguities. The atom coordinates derived from these minimum-function maps were sent through 12 cycles of least-squares refinement.

The structure is based on a new type of silica tetrahedra arrangement which has a silicon to oxygen ratio of 4:10, and which may best be described as a tube of tetrahedra. It consists of four-rings of tetrahedra which are arranged around the 4 axes, with alternating tetrahedra having vertices pointing up and down. The oxygen atoms at these vertices are bonded to similar four-rings above and below, thus forming an endless tube of four rings of tetrahedra in the c direction. Titanium octahedra are bonded together in an infinitely long chain which extends along the four-fold axes. These octahedra are bonded to the tube of tetrahedra through the only oxygen atom of the silica tetrahedra whose bond strength is not completely satisfied by silicon. Irregularly coordinated sodium atoms occupy large voids between the chains and tubes.

The discrepancy factor, R, based on structure factors calculated from the refined atom coordinates, is 14.2 when data with $F_0 = 0$ are included in the computation and 11.5 when they are not. All interatomic distances are close to previously reported values and Pauling's rules are satisfied.

Thesis Supervisor: Martin J. Buerger

Title: Professor of Mineralogy and Crystallography

Table of contents

Abstract	1
List of figures	iv
List of tables	v
Acknowledgements	1
Chapter I Introduction	2
Chapter II Previous work on narsarsukite	4
Chapter III Unit cell and space group	6
Space group	6
Unit-cell dimensions	7
Unit-cell content	9
Chapter IV Measurement of intensities	14
Selection and preparation of material	14
Intensity measurements	14
Chapter V Structure analysis	17
The Patterson synthesis	17
Preliminary considerations	18
Interpretation of the Patterson synthesis	22
Interpretation of the minimum-function maps	34
Chapter VI Refinement	40
Chapter VII Final structure	46
Conformity of narsarsukite to Pauling's rules	54
Bibliography	57

List of figures

	page
figure 1. Diagram of space group $I4/m$, with equipoint locations	8
figure 2. Graphs of unit cell dimensions vs. $\cos^2\theta$	10
figure 3. Harker line $[00z]$	23
figure 4. Minimum-function map based on images of the structure in titanium, with Si:Ti peaks	30
figure 5. Implication map $I4(xy0)$	31
figure 6. Projection on $(xy0)$ of the peaks of the asymmetric unit of the three-dimensional minimum-function which is based on the silicon inversion peak.	36
figure 7. Patterson synthesis $P(xy)$	39
figure 8. Projection of the structure from $z = 0$ to $z = \frac{1}{2}$ on $(xy0)$	47
figure 9. Tube of tetrahedra found in narsarsukite and a simplified version of the same type of arrangement	48
figure 10. Band of silica tetrahedra derived from a mica sheet	50

▼

List of tables

	page
table 1. Analysis of Halfbreed Creek narsarsukite by Ellestad with total iron corrected for FeO and Fe ₂ O ₃ by Schaller	4
table 2. Cell dimensions of all investigators	11
table 3. Derivation of unit-cell contents	13
table 4. Weights of peaks to be expected in Patterson synthesis of narsarsukite assuming half-ionization	19
table 5. Limitations placed on atom positions by equipoint rank	20
table 6. List of equipoints by rank	21
table 7. Patterson levels to be compared to yield the minimum function based on the silicon inversion peak	35
table 8. Coordinates of atoms derived from the minimum-function maps and coordinates and isotropic temperature factors obtained from the refinement	41
table 9. Interatomic distances	52

Acknowledgements

The author is especially indebted to Professor M. J. Buerger who originally suggested the thesis topic and who supervised the entire structure determination. The suggestions offered by all the graduate students in crystallography, including Tibor Zoltai, Charles Prewitt, Charles Burnham and Roberto Poljak, are gratefully acknowledged. Their help in the use of the facilities of the M. I. T. Computation Center was especially appreciated. Specimens were kindly provided by Dr. David B. Stewart of the United States Geological Survey.

Chapter I

Introduction

Before this investigation no work had been done on the crystal structure of narsarsukite. However, certain properties of narsarsukite seemed to indicate possible uniqueness in its crystal structure. It is tetragonal, with two perfect prismatic cleavages ((100)) and ((110)). The silicon to oxygen ratio of its formula (4:11) corresponds to that of the amphibole group of minerals. This combination of symmetry, cleavage and formula is unknown in previously solved crystal structures.

In addition, previous work indicated that a structure determination based on the minimum function method developed by M. J. Buerger would be a good test of this method for two reasons. First, narsarsukite was known to contain 72 atoms in its body-centered cell, which indicates a structure analysis of moderate complexity. Secondly, the presence of the moderately heavy atom titanium makes identification of Patterson peaks much easier than otherwise, thus almost guaranteeing the ultimate solution of the problem.

All material used in this study came from Sage Creek, Montana, and is described in detail by Stewart.⁹

Chapter II

Previous work on narsarsukite

Narsarsukite has been described from only a limited number of localities, which are all in Narsarsuk, Greenland, the original type locality, or the Sweetgrass Hills of Montana. Gossner and Strunz were the first to attempt x-ray studies on the type material.¹ Their results include:

Space group: $C_{4h}^5 = I4/m$

Cell dimensions:

a=10.78 kX units
c= 7.99 kX units

Unit-cell contents:

4($Na_2TiSi_4O_{11}$) with Fe, Mn, and Mg substituting for Ti, and F and OH substituting for O.

Warren and Amberg, working on Greenland material, obtained the following results using single-crystal methods.²

Space group: $S_4^2 = I\bar{4}$, $C_4^5 = I4$, or $C_{4h}^5 = I4/m$

Cell dimensions:

a=10.74 kX units
c= 7.90 kX units

Unit-cell contents:

4($Na_2TiSi_4O_{11}$) with Ti replaced
by minor Fe, Mg, Mn, and Al.

Graham made the original discovery of narsarsukite from Montana.³ An analysis of this material is shown in Table 1.

Table 1

Analysis of Halfbreed Creek narsarsukite by Ellestad with total iron corrected for FeO and Fe₂O₃ by Schaller (after Graham³).

SiO ₂	62.30 %
Al ₂ O ₃	0.32
FeO	0.47
Fe ₂ O ₃	3.13
MgO	0.46
CaO	0.18
Na ₂ O	15.31
K ₂ O	0.41
TiO ₂	16.80
total	99.38 %

A second Montana narsarsukite locality was discovered near Sage Creek by Stewart in 1950 near Graham's original locality.⁹ His crystals showed many forms, and morphological studies resulted in demonstrating that narsarsukite has the point group $4/m$. The center of symmetry (which cannot be determined using x-ray techniques) was confirmed by a negative test for piezoelectricity, etch-pit symmetry, and symmetrical zoning as exhibited by minor color differences. An x-ray powder study gave the following unit cell and space group.

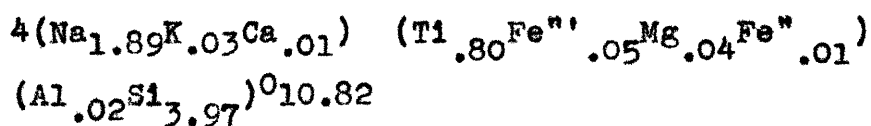
Space group: $I4/m$

Cell dimensions:

$$a = 10.72 \text{ \AA}$$

$$c = 7.948 \text{ \AA}$$

Computations using these cell dimensions, the analysis by Graham on material from his locality, and a specific gravity determination ($\rho = 2.783 \pm 0.014$) resulted in the following unit-cell contents.



Chapter III

Unit cell and space group

A. Space group

Selection of material was especially easy because of the two perfect cleavages of narsarsukite. A small cleavage prism was readily obtained and oriented with the optical goniometer. Precession photographs were taken of several levels in different orientations. The intensity distribution of these photographs corresponded with the diffraction symmetry $4/m\bar{1}-/-$. All reflections could be indexed on the basis of a tetragonal cell with $a=10.77\pm 0.05\text{\AA}$ and $c=7.97\pm 0.05\text{\AA}$. Reflections with $h+k+l=2n+1$ were absent, showing that the cell is body centered. It could not be determined if the true space group of narsarsukite was $I4$, $I4/m$, or $I\bar{4}$ because of the inversion center introduced by x-ray diffraction. To resolve this ambiguity, a single crystal with several forms was chosen and examined under a binocular microscope.

Two lines of evidence indicate that the point group of narsarsukite is $4/m$ and not $\bar{4}$ or 4 . First, there are eight faces which have indices of the general form, (hkl) , and which are about equally developed on the crystal examined. If these faces are symmetrically equivalent, and their equal development suggests this, then they constitute the ditetragonal dipyrmaid form of point group $4/m$. The possibility still exists that these faces represent the equal development of two forms of point group 4 or $\bar{4}$, however.

Second, there is a small pit on (010) which appears to be an etch pit. The only symmetry of this figure is a mirror plane which is normal to the four-fold axis of the crystal. This mirror plane is prohibited by point groups 4 and $\bar{4}$, but required by point group 4/m. There is the possibility, however, that this pit is a growth imperfection. If so, its symmetry might be controlled by the symmetry of the two nearby faces of general indices and it was shown above that these might represent equal development of two forms of symmetry lower than 4/m. Thus the symmetry of the pit might be false.

None of the above evidence is conclusive. In the absence of contrary evidence, however, the space group was taken to be $I4/m$. This is in agreement with the results obtained by Stewart discussed in the previous chapter. A diagram of this space group projected on (xy0) is shown in Fig. 1.

B. Unit-cell dimensions

It was desirable to have more exact unit-cell dimensions, particularly for the computation of reflection directions to be used during the collection of reflection intensities. A crystal was oriented with the optical goniometer and precession camera in preparation for its use in the precision-Weissenberg method of determining unit-cell dimensions.

Equi-inclination

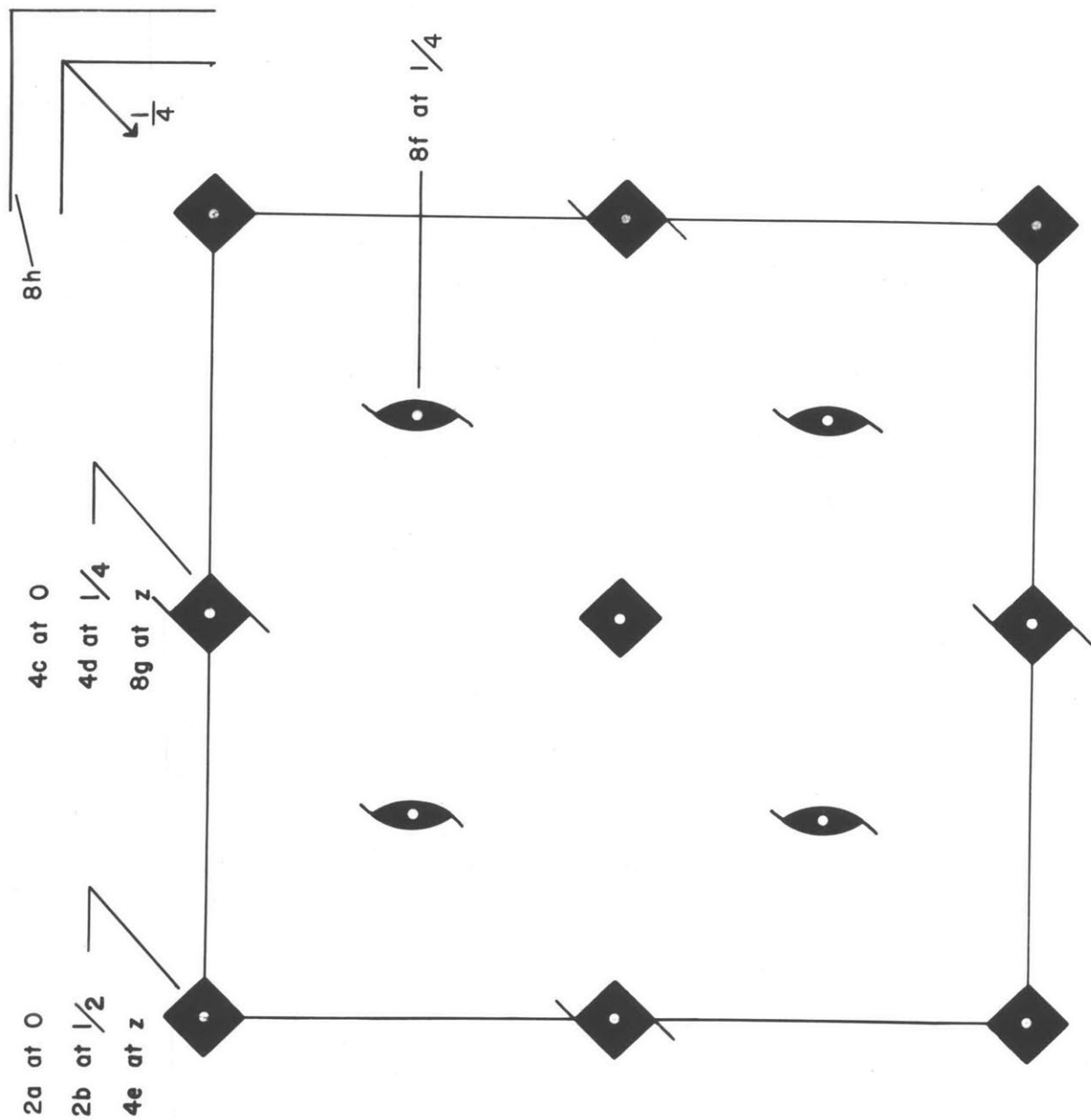


Fig. 1. Diagram of space group $I4/m$ with equipoint locations

Weissenberg photographs of all levels normal to c which were within recording range (levels 0-6) were first taken, since these would be needed as reference in later intensity determinations. The crystal was then transferred to the precision-Weissenberg camera and two photographs (each with the crystal in a different orientation) were taken which allowed very accurate determination of the unit-cell dimensions. Plots of a and c versus $\cos^2\theta$ were prepared and are shown in Fig. 2. As $\cos^2\theta$ approaches 0, the spacing approaches the true value. The precision value of a was needed to compute values of c for the different values of $\cos^2\theta$. Thus the original inaccuracy in a was introduced into the value of c . This dimension could therefore not be determined with as great accuracy as the former. The results of this determination along with those of other investigators are tabulated in Table 2. All results are consistent and within experimental error.

C. Unit-cell content

The unit cell content was determined using the standard relation $nM = \rho VN$, where:

n = number of formula weights per cell

m = weight in grams of one formula weight

ρ = density, g./cc.

V = volume of unit cell in \AA^3

N = Avogadro's number, 6.023×10^{23}

Data used included:

1. a specific gravity of $2.783 \pm .014$ g./cc. as determined by Stewart on Sage Creek material.

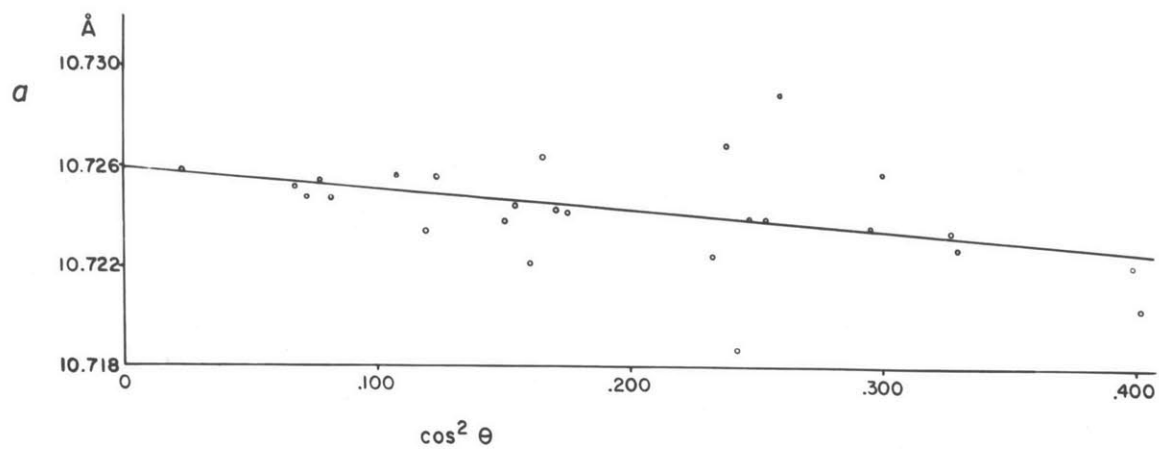
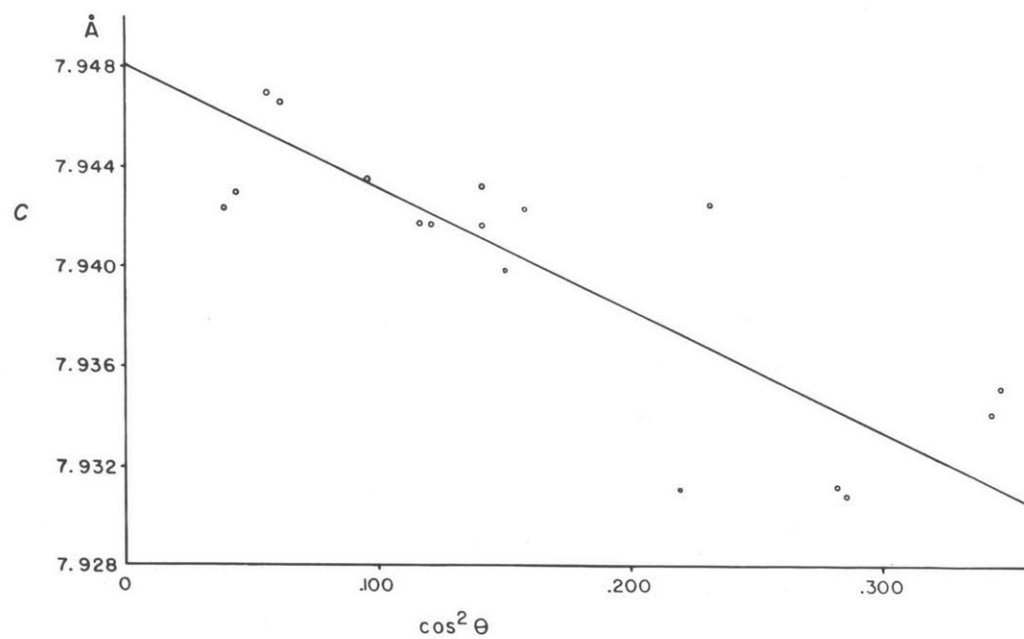
Fig. 2a. Graph of a vs. $\cos^2 \theta$ Fig. 2b. Graph of c vs. $\cos^2 \theta$

Table 2

Cell dimensions of all investigators

	a	c
Gossner and Strunz	10.80 Å*	8.01 Å*
Warren and Amberg	10.76*	7.92*
Stewart	10.72 ₀	7.94 ₈
Peacor	10.726 ₀	7.94 ₈

* kX converted to Å

2. the analysis on Halfbreed Creek, Montana material (Table 1).

3. the unit-cell dimensions of this investigation.

Table 3 shows the results of the computations.

These data yield the following unit-cell formula:

Na 7.58	Ti 3.22	Si 15.90	O 43.48
K 0.14	Fe ^{III} 0.60	Al 0.10	
Ca 0.05	Fe ^{II} 0.18	16.00	
<u>7.77</u>	<u>0.10</u>		
	4.10		

The atom subscripts are all close to multiples of 4, the factor required for all equipoints of space group $I4/m$ with the exception of two of rank two. The excess of the subscript 4.10 over 4.00 plus the deficiency of 7.77 under 8.00 suggests that some iron or magnesium is substituting for sodium. This is very unlikely, however, because of the differences in ionic radii and charges. The discrepancies can be easily explained by inaccuracies in density determinations and chemical analysis. In addition, the analysis was on material from a different locality than that used for the density and unit-cell-dimension determinations. The ideal simplest formula is $\text{Na}_2\text{TiSi}_4\text{O}_{11}$. The subsequent structure determination showed that the formula should actually be written $\text{Na}_2\text{TiOSi}_4\text{O}_{10}$, since one oxygen is coordinated only by titanium. The above data are in agreement with those of other investigators.

Table 3
Calculation of unit-cell contents

$$\rho V \times 6.023 \times 10^{23} = nM = 1533$$

Weight per cent	Weight per cent \times cell mass	"Molecular weight" of oxide	Number of "molecules" of oxide	Number of metal atoms per cell	Number oxygen per ce
62.30%	955.1	60.06	15.90	15.90	31.80
0.32	4.9	161.96	0.05	0.10	0.15
0.47	7.2	71.85	0.10	0.10	0.10
3.13	48.0	159.70	0.30	0.60	0.90
0.46	7.1	40.32	0.18	0.18	0.18
0.18	2.8	56.08	0.05	0.05	0.05
15.31	234.7	62.00	3.79	7.58	3.79
0.41	6.3	94.20	0.07	0.14	0.07
16.80	257.5	79.90	3.22	3.22	6.44
<hr/>					<hr/>
99.38					43.48

Chapter IV

Measurement of intensities

A. Selection and preparation of material

In order to assure maximum accuracy in intensity determinations the selection of a crystal was made with great care. An ideal sample must meet two requirements. First, the crystal must be as small as possible to bring absorption down to a minimum. Secondly, it should be perfectly cylindrical so that absorption corrections may be easily and accurately made. The final crystal chosen was a cleavage fragment. Because of the development of the ((100)) and ((110)) cleavages this was a nearly cylindrical prism .031 mm. in diameter and .250 mm. long. This was so small that orientation with the optical goniometer was only approximate because reflections from the cleavages were nearly undetectable. Final perfect orientation was achieved with the precession camera. The crystal was then transferred to the Geiger-counter apparatus.

B. Intensity measurements

All intensities were measured with the single-crystal Geiger-counter diffractometer. The crystal setting and the Geiger setting for each reflection were obtained using a computer program prepared by Mr. Charles Moore of these laboratories. Computations were made on the I. B. M. 704 computer at the M. I. T. Computation Center.

This program also gave corrections for the Lorentz and polarization factors, as well as values of $\sin \Theta$, for each reflection.

Special care was taken to confine the intensities to the linearity range of the Geiger counter. Aluminum foils were used to decrease the reflection intensities when they were greater than about 120 counts per second. These foils were carefully calibrated for their absorptions. In order to keep almost all of the reflections below a counting rate of 120 counts per second a very low voltage was used. This unfortunately resulted in such low intensities that approximately 15 % of the reflections were below the recording range of the Geiger counter. However, since a very low voltage was used, the most intense reflections had intensities which fell well within the the absolute linearity range of the Geiger counter. It was hoped that this gain in accuracy in measurement of high intensity reflections would make up for the loss of data on reflections of very low intensity.

There are about 480 reflections in the asymmetric unit of the copper reciprocal sphere of narsarsukite, but only 469 were within the recording range of the apparatus. These reflections were measured and corrected for the necessary factors. The Lorentz and polarization corrections were provided as noted above by an I. B. M.

704 computer program. The linear absorption coefficient was based on the analysis of Graham's Montana narsarsukite. Absorption corrections were made according to the theory developed for a cylindrical specimen by Buerger and Niizeki.⁵ The corrected intensities were then ready for use as Fourier coefficients in a Patterson synthesis.

Chapter V

Structure analysis

It was decided that a two-dimensional Patterson projection would contain too many coalescing peaks since narsarsukite is a mineral of moderate complexity (72 atoms in the body-centered cell). Therefore, it was planned to solve the structure by applying the minimum function to the three-dimensional Patterson synthesis, which was sure to contain very few coalescing peaks.

A. The Patterson synthesis

The three-dimensional Patterson synthesis was computed on the I. B. M. 704 computer at the M. I. T. Computation Center using MIFRI,⁸ a standard program for computing Fourier series. Since the Patterson synthesis has symmetry $4/m$ and the cell is body centered, it was only necessary to obtain the synthesis for one sixteenth of the volume of the unit cell. This asymmetric unit was obtained in sections normal to c , with Patterson values computed at intervals of $1/60$ along all three axes. The section was computed with z varying from $0/60$ to $15/60$, and x and y varying from $0/60$ to $30/60$.

Using the height of the origin peak obtained in the synthesis as a guide, the heights of peaks on the Patterson maps were computed. These are shown in

Table 4. In order to determine the height of the peaks it is first necessary to choose an absolute-zero level on the Patterson maps. Since this choice may be subject to a fairly large error, this same error will be inherent in the computation of the expected peak heights shown in Table 4. The correlation between expected peak heights and peak heights actually found may be somewhat inaccurate because of this.

B. Preliminary considerations

Comparison of the ranks of the various equipoints of space group $I4/m$ with the number of each kind of atom in the unit cell places initial restrictions on some atom positions. The possible positions are listed in Tables 5 and 6. All equipoints have one of the ranks 2, 4, 8, or 16. Since no combination of 16 and 8 will yield 44, the total number of oxygen atoms in the unit cell, at least four of the oxygen atoms must be located on an equipoint of rank four or on two equipoints of rank two. Therefore at least four oxygen atoms must occupy one of the equipoints 4e, 4d, 4c, or 2a and 2b. Since there are only four titanium atoms in the unit cell, titanium must also occupy one of these equipoints. Equipoints 4c and 4d are on the $\bar{4}$ axes while 4e, 2a, and 2b are on the 4-fold axes. It is possible that both oxygen and titanium occupy the same set of axes. For example titanium might occupy position 4c and

Table 4

Weights of peaks to be expected in Patterson
synthesis of narsarsukite assuming half ionization.

$$\sum z^2 = 4175$$

Peak due to atom pair	$Z_1 \times Z_2$	Approximate height of peak expected with an origin peak height of 2150	
		Single peak	Double peak
Tl:Tl	20 x 20=400	206	412
Si:Si	12 x 12=144	74	148
Na:Na	10.5 x 10.5=110.25	57	114
O:O	9 x 9=81	42	84
Tl:Si	20 x 12=240	124	248
Tl:Na	20 x 10.5=210	108	216
Tl:O	20 x 9=180	93	186
Si:Na	12 x 10.5=126	65	130
Si:O	12 x 9=108	56	112
Na:O	10.5 x 9=94.5	49	98

Table 5

Limitations placed on atom positions by
equipoint rank

Atom	Number in cell	Possible equipoint rank distributions																								
Ti	4	4 2 2																								
Na	8	8 4 4 4 2 2																								
Si	16	16 8 8 8 4 4 8 4 2 2 4 4 4* 2 2																								
O	44	<table border="0"> <tr> <td>16 16 8 4</td> <td>8 8 8 8 8 4</td> </tr> <tr> <td>16 16 8 2 2</td> <td>8 8 8 8 8 2 2</td> </tr> <tr> <td>16 16 4 4 4</td> <td>8 8 8 8 4 4 4</td> </tr> <tr> <td>16 16 4 4 2 2</td> <td>8 8 8 8 4 4 2 2</td> </tr> <tr> <td>16 8 8 8 4</td> <td>8 8 8 4 4 4 4 4</td> </tr> <tr> <td>16 8 8 8 2 2</td> <td>8 8 8 4 4 4 4 2 2</td> </tr> <tr> <td>16 8 8 4 4 4</td> <td>8 8 4 4 4 4 4 4 4</td> </tr> <tr> <td>16 8 8 4 4 2 2</td> <td>8 8 4 4 4 4 4 4 2 2</td> </tr> <tr> <td>16 8 4 4 4 4 4</td> <td>8 4 4 4 4 4 4 4 4 4</td> </tr> <tr> <td>16 8 4 4 4 4 2 2</td> <td>8 4 4 4 4 4 4 4 2 2</td> </tr> <tr> <td>16 4 4 4 4 4 4 4</td> <td>4 4 4 4 4 4 4 4 4 4 4</td> </tr> <tr> <td>16 4 4 4 4 4 4 2 2</td> <td>4 4 4 4 4 4 4 4 4 4 2 2</td> </tr> </table>	16 16 8 4	8 8 8 8 8 4	16 16 8 2 2	8 8 8 8 8 2 2	16 16 4 4 4	8 8 8 8 4 4 4	16 16 4 4 2 2	8 8 8 8 4 4 2 2	16 8 8 8 4	8 8 8 4 4 4 4 4	16 8 8 8 2 2	8 8 8 4 4 4 4 2 2	16 8 8 4 4 4	8 8 4 4 4 4 4 4 4	16 8 8 4 4 2 2	8 8 4 4 4 4 4 4 2 2	16 8 4 4 4 4 4	8 4 4 4 4 4 4 4 4 4	16 8 4 4 4 4 2 2	8 4 4 4 4 4 4 4 2 2	16 4 4 4 4 4 4 4	4 4 4 4 4 4 4 4 4 4 4	16 4 4 4 4 4 4 2 2	4 4 4 4 4 4 4 4 4 4 2 2
16 16 8 4	8 8 8 8 8 4																									
16 16 8 2 2	8 8 8 8 8 2 2																									
16 16 4 4 4	8 8 8 8 4 4 4																									
16 16 4 4 2 2	8 8 8 8 4 4 2 2																									
16 8 8 8 4	8 8 8 4 4 4 4 4																									
16 8 8 8 2 2	8 8 8 4 4 4 4 2 2																									
16 8 8 4 4 4	8 8 4 4 4 4 4 4 4																									
16 8 8 4 4 2 2	8 8 4 4 4 4 4 4 2 2																									
16 8 4 4 4 4 4	8 4 4 4 4 4 4 4 4 4																									
16 8 4 4 4 4 2 2	8 4 4 4 4 4 4 4 2 2																									
16 4 4 4 4 4 4 4	4 4 4 4 4 4 4 4 4 4 4																									
16 4 4 4 4 4 4 2 2	4 4 4 4 4 4 4 4 4 4 2 2																									

* Where 3 or more positions of rank 4 appear all
but two must be equipoint 4e.

Table 6

List of equipoints by rank

rank	equipoints
2	2a, 2b
4	4c, 4d, 4e
8	8f, 8g, 8h
16	16i

oxygen position 4d. Reference to the space group diagram (Fig. 1) shows that this distribution consists of strings of alternating titanium and oxygen atoms. Titanium atoms would be located along the $\bar{4}$ axes at $z = 0/60, 30/60,$ and $60/60$ while oxygen atoms would be at $z = 15/60$ and $45/60$. Thus the interval between titanium and oxygen atoms would be $15/60 = c/4$. The observed $c/4$ distance (1.99 \AA) compares favorably with known Ti-O distances (e.g. 1.96 \AA),⁴ strongly suggesting that this type of titanium-oxygen distribution is correct. There are four possible arrangements of the strings of alternating titanium and oxygen atoms, however, each corresponding to a combination of the equipoints given above. Each arrangement yields a Ti-O distance of $c/4$.

C. Interpretation of the Patterson synthesis

A plot of the Harker line $[00z]$ from $z = 0$ to $z = 30/60$ is shown in Fig. 3. Peaks can be distinguished at $z = 23/60, 14/60,$ and $30/60$. Reference to the space group diagram (Fig. 1) showed that the titanium and oxygen atoms which may alternate along the 4 or $\bar{4}$ axes should be separated by an interval of $z = 15/60$. Since there are four oxygen and four titanium atoms per unit cell, there should be a peak of height $4(\text{Ti:O})$ at $z = 15/60$ of the Harker line. Table 4 shows that this height is $4 \times 93 = 372$, which agrees well with the peak of height 380 found at $z = 14/60$ of the Harker line.

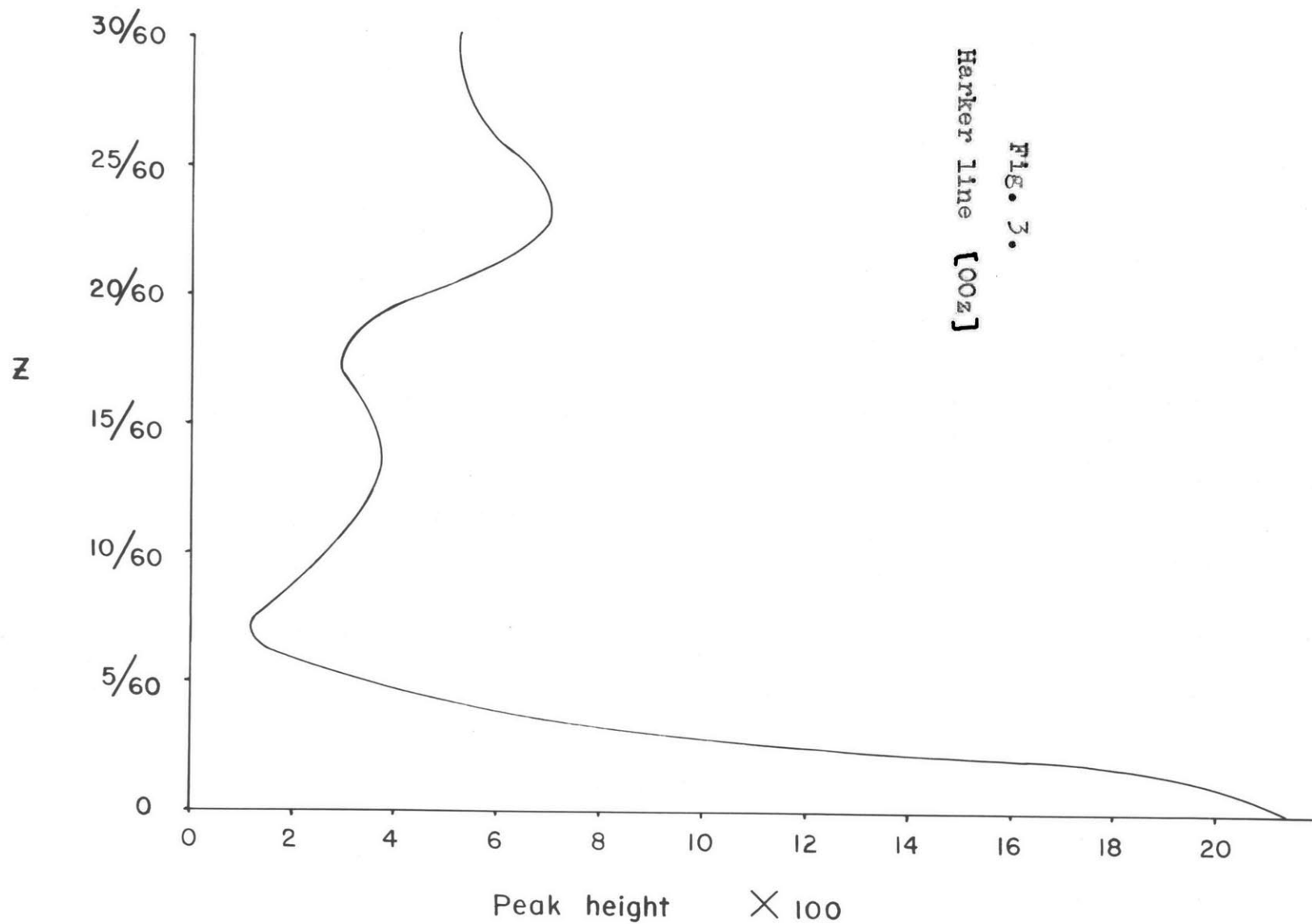


FIG. 3.
Harker line [00z]

In addition, titanium atoms should be separated by an interval of $z = 30/60$, as should oxygen atoms. There should therefore be a peak at $z = 30/60$ of the Harker line with height $2(\text{Ti}:\text{Ti}) + 2(\text{O}:\text{O})$. Table 4 shows this height to be $412+84 = 496$, which is close to the height of 520 actually found. This is consistent with a titanium-oxygen chain distribution along the 4 or $\bar{4}$ axes.

Since the minimum function was to be used in determining the crystal structure, it was necessary to locate an inversion peak in order to begin the image-seeking process. Buerger has shown how to locate inversion peaks through the use of correlation minimum-function maps.⁶ Since this case involves a four-fold axis with a perpendicular mirror plane, an inversion peak can be located on any level z by exactly superimposing level z on level 0 and contouring the minimum function. This was done for all levels from $z = 0$ to $z = 30/60$. If silicon occupies the equipoint with general coordinates, the symmetry $4/m$ should produce a peak of weight $4(\text{Si}:\text{Si})$ on the Harker line on the same level as the silicon inversion peak. Examination of the Harker line had shown one peak which was still unaccounted for at $z = 23/60$. The correlation map of level $z = 23/60$ was therefore thought to offer the best prospect for the location of a silicon inversion peak.

This level does in fact show a strong peak believed to be a possible inversion peak, as well as its expected rotation-equivalent peak. The heights of these two peaks are several times greater than the computed expected values of the silicon peaks, showing that they are multiple peaks. A minimum-function solution based on a multiple peak yields a multiple solution, so these peaks could not be used in the minimum-function image seeking process. It was decided to attempt to find an inversion peak by another process, since no other candidate inversion peaks could be located by the correlation minimum-function method.

Another procedure was suggested by the restrictions placed on the titanium locations by the equipoint distribution. The possible titanium locations are listed in Table 5. All coordinates of equipoints 2a, 2b, 4c, and 4d are fixed, but the z coordinate of equipoint 4e is variable. Reference to the space group diagram shows that the probable titanium-oxygen chain distribution suggested above requires this coordinate to be $15/60$, since the titanium atoms must be separated by an interval of $z = 30/60$. With this qualification, it can easily be seen from the space-group diagram that all four possible titanium distributions differ from each other only in the location of the origin. This requires that the Patterson-peak distribution

resulting only from Ti:Ti vectors be the same for all four cases. Therefore it is not possible to ascertain which distribution is the correct one merely by noting the locations of the high Ti:Ti peaks on the Patterson maps. Since, in all four possible distributions, titanium atoms lie on the 4 or $\bar{4}$ axes separated from one another by an interval of $z = 30/60$, a method is available for readily solving the structure. Consider, first, only two of the titanium atoms of one of the possible equipoint distributions, separated only by an interval of $z = 30/60$. The Patterson maps contain an image of the crystal structure in both of these atoms. If these two images can be brought together and the minimum function mapped, the result will be an approximation to the crystal structure. In particular, if all Patterson maps differing by an interval $z = 30/60$ are exactly superimposed and the minimum function mapped, the correct solution results. Notice that it makes no difference where the two titanium atoms are located in the actual structure, just as long as they lie one above the other separated by the given interval. There are, however, ambiguities in the minimum-function solution described above. First, oxygen atoms are distributed like the titanium atoms (on the 4 or $\bar{4}$ axes separated by an interval of $z = 30/60$). There is also an image of the structure in the oxygen atoms. The above mapping

procedure will therefore yield a solution based on these images, superimposed on the solution based on the images of the structure in the titanium atoms. This should cause little difficulty however, since the Patterson peaks based upon titanium as an image point far out-weigh peaks based upon oxygen. The minimum-function solution will thus contain high peaks representing the structure. Superimposed on these will be a ghost due to the structure seen from the oxygen atoms.

A second ambiguity in the minimum-function maps is caused by the presence of a false inversion center with coordinates $x = \frac{1}{4}$, $y = \frac{1}{4}$ in each level of the minimum function. An ambiguity of two thus results in the location of each atom. This ambiguity is caused by the centering translation of the unit cell. Consider the two titanium atoms upon which the minimum-function solution is to be based. These are located one above the other separated by an interval of $z = 30/60$. Now refer to the space group diagram. In all possible titanium distributions, it can be seen that these first two atoms are related to a similar pair by the component of the unit-cell centering translation which is normal to c . These second two atoms are also located one above the other, separated by an interval of $z = 30/60$. The Patterson maps also contain images of the structure in the pair of atoms. The images seen by each pair

of atoms are therefore related by this translation, which is equivalent to an inversion center at $x = \frac{1}{4}$, $y = \frac{1}{4}$ of each level. The result produced by comparing any two Patterson levels separated by an interval of $z = 30/60$ is a minimum-function map with a double solution to the structure. One solution is related to the other by the component of the centering translation normal to c , which is equivalent to an inversion center at $x = \frac{1}{4}$, $y = \frac{1}{4}$ for each level of the minimum function.

A third problem is the lack of knowledge of the absolute origin in the minimum-function maps. The titanium atom will be represented by a high peak at the origin of one of the minimum-function maps. But there are four possible equipoints where the titanium may be located and only one of these includes the real origin of the crystal. The set of minimum-function maps will contain the true solution to the structure, but the absolute unit-cell coordinates of the atoms will depend on the placement of this set of maps in crystal space. If the titanium atom can be given its true location, then the set of minimum-function maps may be given their true placement and the absolute coordinates of the atoms will be known.

The minimum-function mapping procedure outlined above was carried out for the asymmetric unit of the unit cell, by using two titanium atoms as image points.

Levels of the Patterson function separated by an interval of $z = 30/60$ were compared. Levels $0/60$ to $15/60$ were successively compared with levels $30/60$ to $45/60$ to yield a set of 15 minimum-function maps. These maps contain, of course, the ambiguities discussed above. A high peak of the expected weight representing the titanium atom is at the origin. It was only necessary then to determine which position of the four possibilities that this titanium occupied, to give the entire set of minimum-function maps their correct placement in crystal space. Only one large peak and its inversion equivalent was found to have general coordinates (Fig. 4). Since silicon is the only relatively heavy atom which may have general coordinates (Table 5), this peak height (320) was compared with the computed expected height of the silicon peak. This height $2(\text{Si}:\text{Ti}) = 248$ is close to the height actually found. The location of the silicon atom was thus determined relative to the titanium atom, with the exception of the ambiguity due to the inversion center.

An implication map $I_4(xy0)$ was next prepared (Fig. 5). This is a projection of an approximation to the crystal structure, with ambiguities, on $(xy0)$. There are high peaks on this map corresponding to all possible titanium positions. Since this map is a projection, equipoints $4c$ and $4d$ are projected to $0, \frac{1}{2}, 0$.

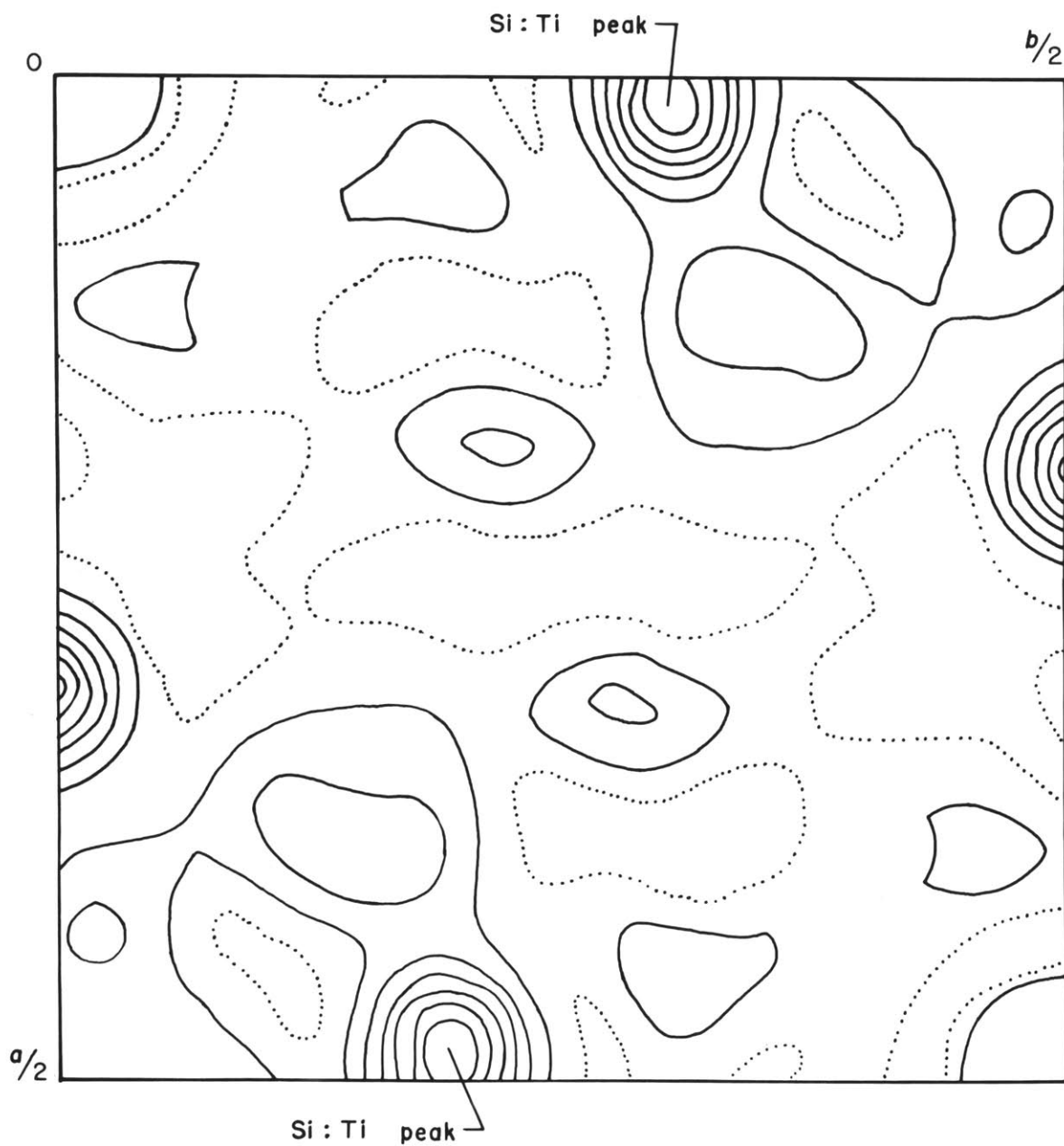


Fig. 4. Minimum-function map based on images of the structure in titanium, with Si:Ti peaks

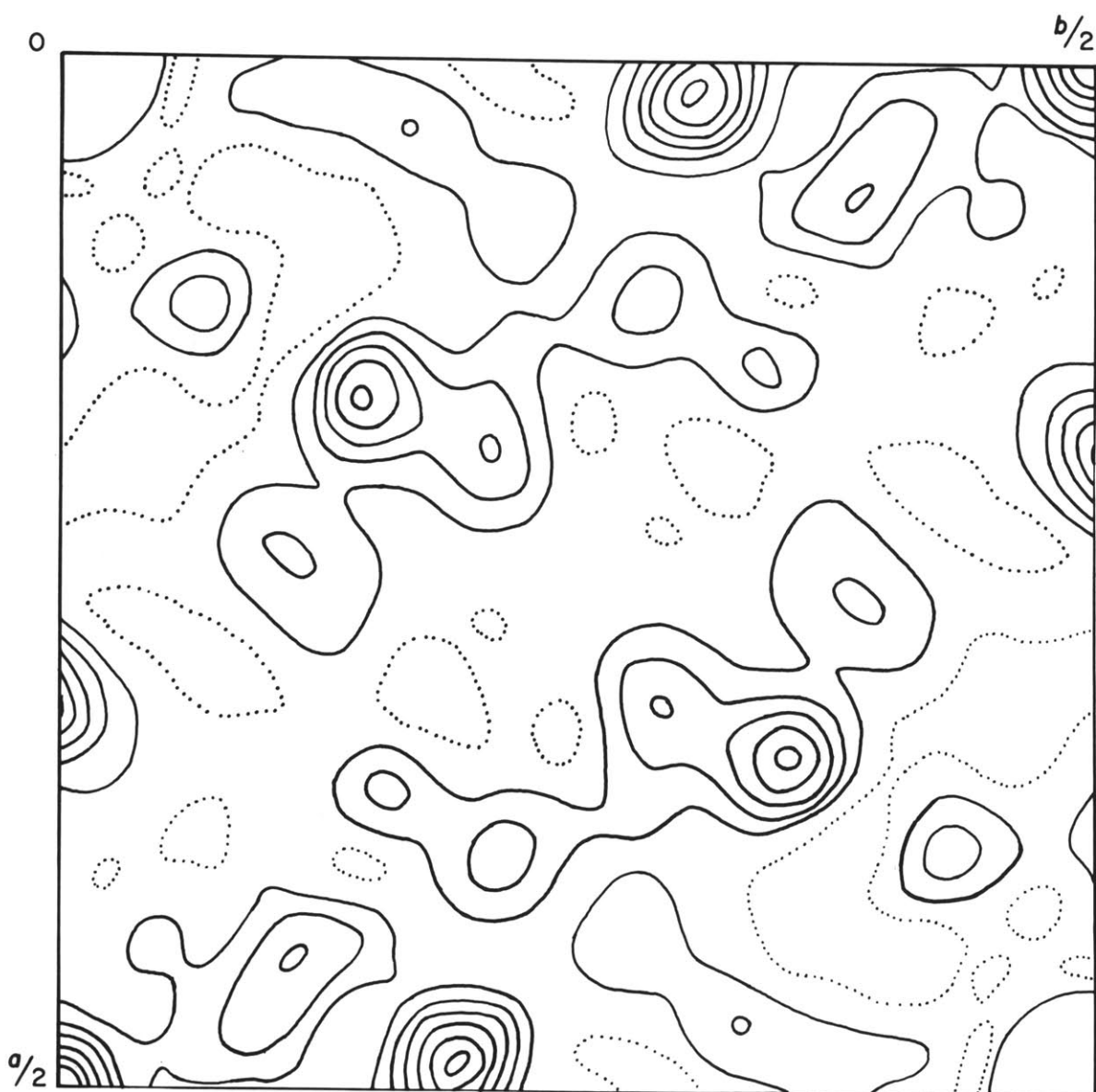


Fig. 5.

Implication map $\Pi_4(xy0)$

It is possible that the titanium atoms are located on one of these two equipoints. The set of minimum-function maps was placed so that the high titanium peak of these maps was superimposed on the high peak at $0, \frac{1}{2}, 0$ of the implication map. Since each type of map is an approximation to the crystal structure, there should be good correlation of high peaks, if the titanium atom is located at equipoint 4c or 4d. There is, however, no peak on the implication map corresponding to either of the possible silicon peaks on the minimum-function maps. The possible titanium positions 4c and 4d are thus eliminated. The other positions which the titanium may occupy (4e, 2a, 2b) are located at $0, 0, 0$ of the implication map. Minimum-function maps were placed over the implication maps so that the high titanium peak was superimposed on the high peak at $0, 0, 0$ of the implication map. There is good correlation, not only of the silicon peaks, but of all minimum-function peaks, with implication peaks. The titanium atoms are thus located either on equipoint 4e (with $z = 15/60$) or 2a and 2b. In addition, the silicon atom has been determined relative to the titanium atom with the exception of the ambiguity due to the inversion center.

It can easily be seen from the minimum-function maps that the silicon and titanium atoms are separated by an interval of $z = 4/60$. If the titanium is on

equipoint $4e(0,0,15/60)$ the silicon atom is on level $11/60$. This yields a high silicon reflection peak on the Harker line $[00z]$ at $z = 22/60$. There is, in fact, a high peak there, the only one on the Harker line unaccounted for. On the other hand, if the titanium atom is located on equipoint $2a(0,0,0)$, the silicon atom would be on level $z = 4/60$. A high peak would thus appear on the Harker line at $z = 8/60$. The location of a trough in the Patterson function at $z = 8/60$ eliminates this possibility. The titanium atom is thus definitely located at $0,0,15/60$ (equipoint $4e$). Therefore the levels of the minimum function with the titanium atom at the origin can be given their proper placement in crystal space. This locates the silicon atom with an ambiguity due only to the inversion center in the level in which it occurs.

The location of an inversion peak in the Patterson function can easily be predicted if the locations of the atoms causing it are known. Since the silicon atom is on level $11/60$, the inversion peak should occur on level $22/60$. Patterson maps of levels close to $z = 22/60$ were inspected to see if the silicon peak could be found in the predicted location. There are, in fact, inversion peaks of the correct weight corresponding to each of the two possible silicon-atom locations. Using one of these inversion peaks, a

complete set of minimum function maps of the asymmetric unit was prepared. The Patterson superpositions are listed in Table 7. The initial superpositions resulted in M_2 maps but these could be combined with themselves using the four-fold axis to obtain M_8 maps which are a good approximation to the electron density. This same procedure was carried out using the other possible silicon inversion peak as the starting point for the image-seeking process. It was noticed, however, that the set of maps obtained in this case was exactly the same as that based on the other inversion peak, differing from it only in the location of the origin.

D. Interpretation of the minimum-function maps.

A projection on (xyO) of the peaks of the three-dimensional minimum-function maps based on the silicon inversion peak is shown in Fig. 6. Only peaks in the interval $z = 0$ to $\frac{1}{4}$ are shown. The large peak at the origin with coordinates $0, 0, \frac{1}{4}$ is, of course, the titanium peak. The smaller peak at the origin with $z = 0$ is an oxygen peak, (O_I) whose location was suggested above by the titanium-oxygen chain hypothesis. In addition, the peak at $\frac{1}{2}, \frac{1}{2}, 0$ represents the other oxygen atom (O_{II}) whose location was suggested. The silicon peak which served as the basis of the image-forming function is marked with a cross. The next highest peak is located on level

Table 7

Patterson levels to be compared to yield the minimum function based on the silicon inversion peak.

Levels to be compared	Levels which are equivalent by Patterson symmetry	Resulting minimum-function level
27, 4	3, 4	15.5
26, 3	4, 3	14.5
25, 2	5, 2	13.5
24, 1	6, 1	12.5
23, 0	7, 0	11.5
22, -1	8, 1	10.5
21, -2	9, 2	9.5
20, -3	10, 3	8.5
19, -4	11, 4	7.5
18, -5	12, 5	6.5
17, -6	13, 6	5.5
16, -7	14, 7	4.5
15, -8	15, 8	3.5
14, -9	14, 9	2.5
13, -10	13, 10	1.5
12, -11	12, 11	0.5
11, -12	11, 12	-0.5

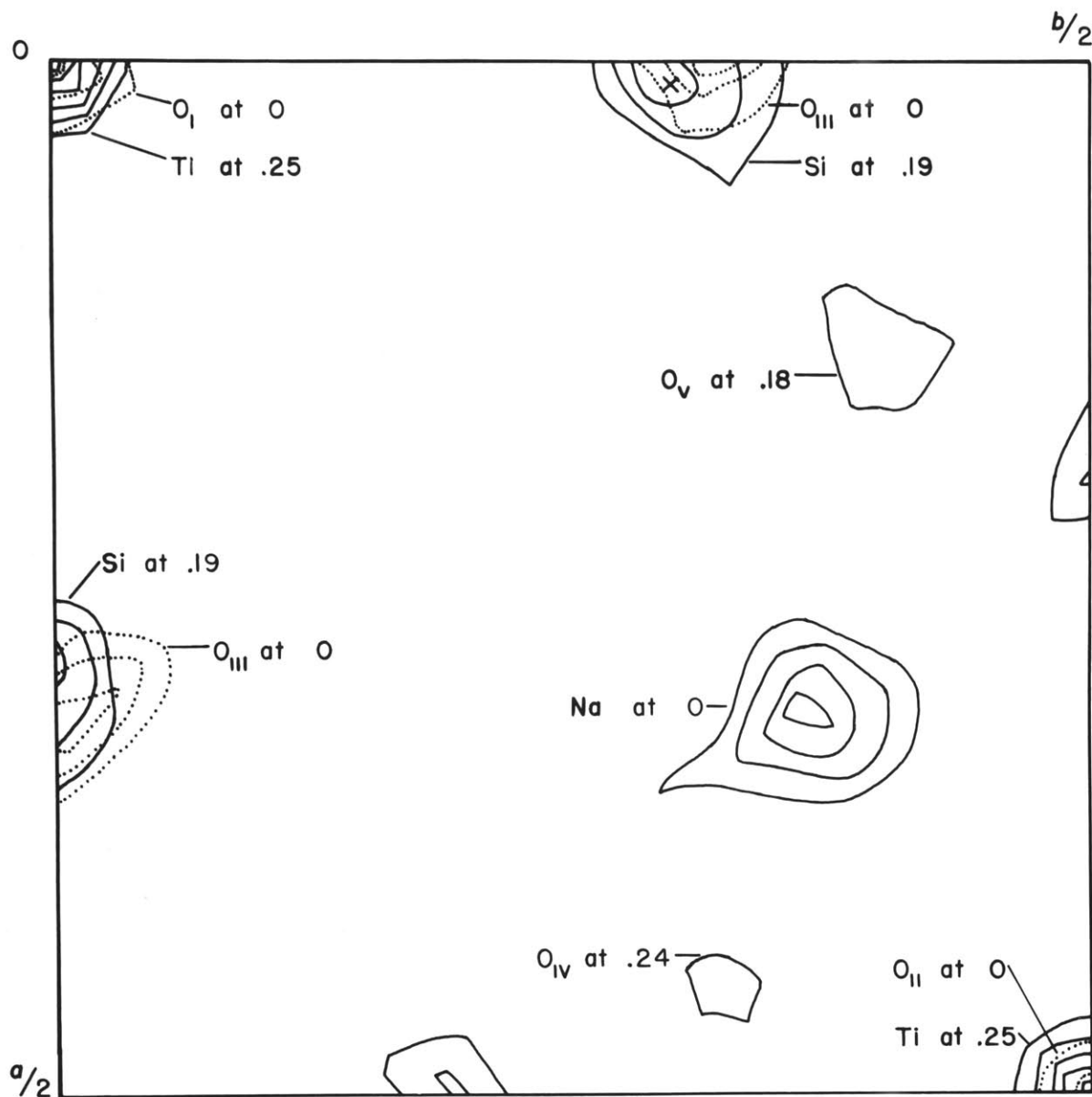


Fig. 6.

Projection on $(xy0)$ of the peaks of the asymmetric unit of the three-dimensional minimum-function which is based on the silicon inversion peak

$z = C$, a position of rank 8. Since there are 8 sodium atoms in the unit cell this relatively heavy peak must represent a sodium atom. This then locates all cations and four oxygen atoms with no ambiguities.

Forty oxygen atoms still remain to be located. Four peaks, three of rank 16 and one of rank 8, remain on the minimum-function peak projection. All of these are peaks of low weight and have close to the expected oxygen-peak height. Two of the peaks of rank 16 and the peak of rank 8, when repeated by symmetry operations, complete tetrahedral coordination for silicon and yield Si-O distances close to standard values. In addition, titanium has its usual octahedral coordination and all Ti-O distances are close to values found in other structures. These three peaks were therefore taken to be approximations to the electron density of oxygen atoms. They are labeled O_{III}, O_{IV}, and O_V in the projection of the minimum-function peaks. This completes the location of all atoms of the unit cell. One false minimum-function peak remains unlabeled.

Four checks were made of the correctness of the proposed structure. First, comparison with the implication diagram shows good correlation of implication peaks with minimum-function peaks. Second, the original set of minimum-function maps based on titanium shows one-to-one peak correlation with the maps based

on the silicon inversion peak (with the exception of the ambiguity due to centrosymmetry in the former maps). Third, a two-dimensional Patterson projection $P(xy)$ was prepared. Since the titanium atom is located at $0,0,\frac{1}{2}$, and since Patterson peaks involving the relatively heavy titanium atom should dominate this map, it should be a rough approximation to a projection of the crystal structure. This map was prepared using the I. B. M. 704 computer at the M. I. T. Computation Center in conjunction with the Fourier series computation program MIFRI.⁸ It is shown in Fig. 7. There is good peak correlation again. Fourth, all cation-anion distances compare well with distances previously recognized in other crystal structures.

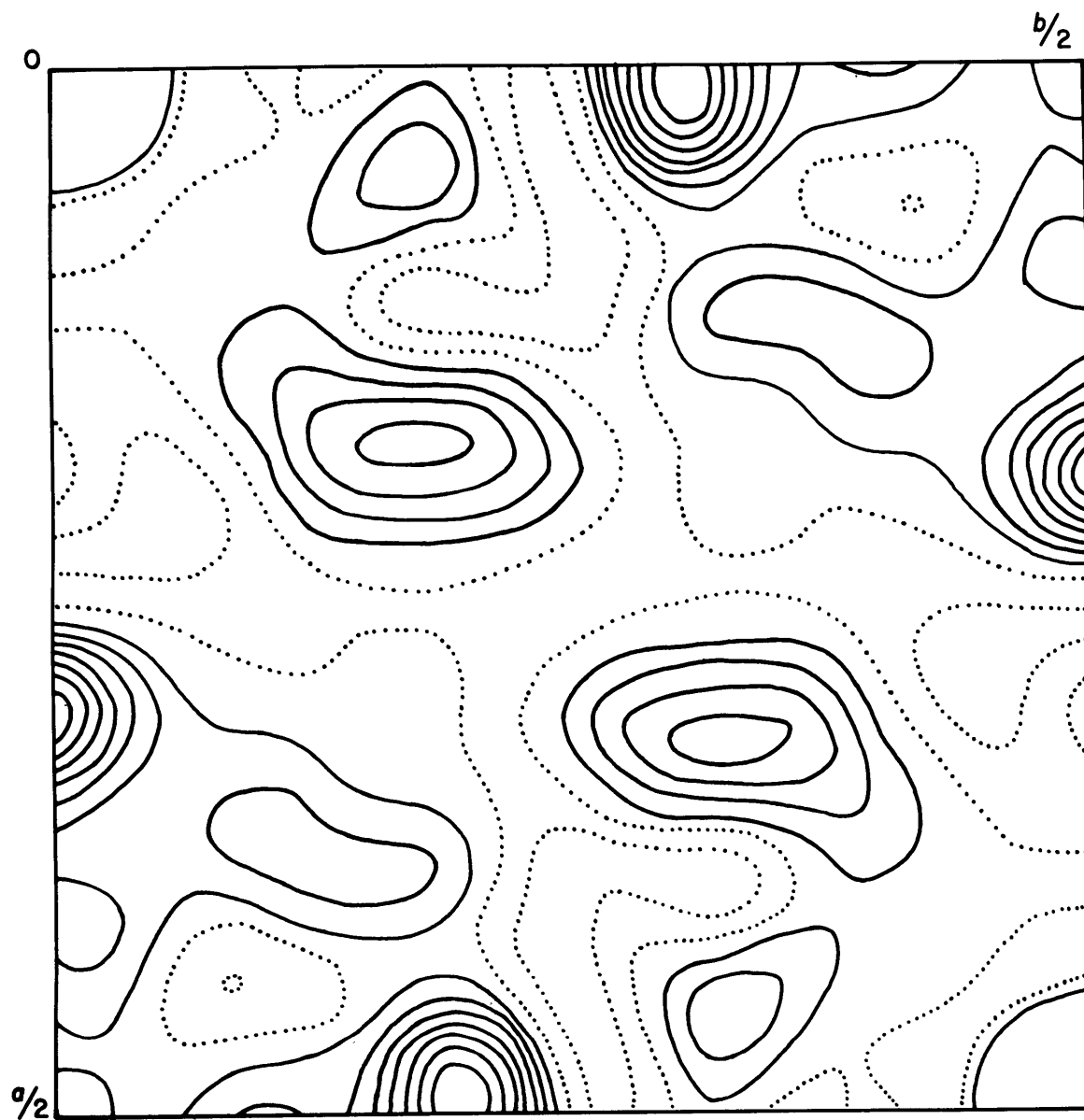


Fig. 7.

Patterson synthesis $P(xy)$

Chapter VI

Refinement

Refinement of the atom parameters of narsarsukite was carried out using the Busing and Levy least-squares program on the I. B. M. 704 computer at the M. I. T. Computation Center. This program permits simultaneous refinement of all atom coordinates, temperature factors (overall, individual isotropic, or individual anisotropic) and one or more scale factors. It computes structure factors and the discrepancy factor, R , based on input parameters. Therefore, in order to compute a discrepancy factor for the parameters obtained as the output for a given cycle, a separate computation or another cycle must be run.

The coordinates of the atoms of narsarsukite derived from the minimum-function map based on the silicon inversion peak are tabulated in the first section of Table 8. These were used as input data for the first cycle of refinement along with the following data:

1. An arbitrary scale factor of 1.0
2. All F_o , including data with $F_o = 0$
3. An arbitrary value of 0.7 for all individual temperature factors
4. Form factors assuming half-ionization

Six cycles were run in which only the scale factor and the atom coordinates were allowed to refine. The refined

Table 8

Coordinates of atoms derived from the minimum-
function maps and coordinates and isotropic
temperature factors obtained from the refinement

Atom	Coordinates derived from minimum- function maps			Coordinates and isotropic temperature factors obtained from refinement			
	x	y	z	x	y	z	B
Tl	0	0	.250	0	0	.239	1.2 Å ³
Na	.186	.141	$\frac{1}{2}$.186	.138	$\frac{1}{2}$	1.9
Si	.008	.294	.192	.012	.308	.191	.2
O _I	0	0	0	0	0	0	.9
O _{II}	0	0	$\frac{1}{2}$	0	0	$\frac{1}{2}$.5
O _{III}	-.009	.316	0	-.038	.301	0	.8
O _{IV}	.055	.179	.250	.049	.177	.268	.6
O _V	.128	.392	.183	.133	.403	.192	.6

atom coordinates and scale factor of each cycle were used as input data for the next cycle. All other input data, including the individual temperature factors, remained unchanged. The largest change in the fractional coordinate of the atoms during the sixth cycle was 2×10^{-4} . The stage of the refinement during which the temperature factors were held constant was therefore regarded as completed. The individual isotropic temperature factors, along with the atom coordinates and scale factor, were allowed to vary in all subsequent cycles. The temperature factor of O_{II} obtained from cycle 7 was negative. The least-squares program does not refine if negative temperature factors are used as input data, so a method was sought to resolve this difficulty.

The points of a plot of $\ln F_o/F_c$ vs. $\sin^2 \theta$ should lie approximately along a straight line with a slope which is a function of the overall temperature factor if values of F_c are based on the correct structure. The intersection of the line with the $\ln F_o/F_c$ axis provides the scale factor. With perfect experimental intensity data and perfectly refined atom coordinates, all points of the plot fall exactly on a straight line. The distance of a point from the line is a rough measure of the accuracy of F_c . It was believed that the negative temperature factor obtained in cycle 7 was

caused by inaccurate intensity data, and that the type of plot described above would confirm this. In preparation for such a plot, values of F_o for all reflections were computed using a temperature factor of zero and atom parameters of cycle 6. Values of $\sin \theta$ for each reflection were provided by the I. B. M. 704 program which had also provided Lorentz and polarization factors, etc.. The resulting plot showed a wide scatter of points, which indicated that some data were inaccurate, but there was a majority of points which occupied a wide band with a negative slope. Arbitrary border lines were drawn outlining this band, with approximately 130 points falling outside of these limits. It was believed that these represented the most inaccurate data, and might have caused the temperature factor of O_{II} obtained from cycle 7 to be negative. Only those reflections which fell within the band limits were used as input data for cycle 9 (340 reflections). A small positive number (0.20) was used for the temperature factor of O_{II} and all parameters were allowed to vary. During this cycle all temperature factors remained positive, confirming the fact that the inaccurate data had been responsible for the negative temperature factor.

The points of a plot of $\ln F_o/F_c$ vs. $\sin^2\theta$ should lie approximately along a straight line with negligible

slope after correcting for the temperature factor. Since the line now had zero slope, a data rejection test other than the one described above could be used. Mr. Charles Prewitt prepared a patch for the least-squares program which allowed only those data with $|F_o - F_c|/F_o < 0.25$ to be included in the refinement. This rejection test has essentially the same effect as the one used in cycle 9, in that it includes data in the refinement process which occupy a wide band on the plot of $\ln F_o/F_c$ vs. $\sin^2 \theta$. It has the advantage of allowing all reflections, whether used in the refinement process or not, to be included in the input data deck and therefore to be included in the calculation of the discrepancy factor. This rejection test also excluded data with $F_o \approx 0$ (approximately 15% of the reflections) from the refinement process.

Cycles 10, 11 and 12 were run using the new rejection test, permitting all parameters to vary. After cycle 11 it was discovered that incorrect weights had been applied to the reflection data. All reflections had been weighted equally, when in fact, all zero-level reflections have a multiplicity one half that of reflections of general indices. Cycle 12 was accordingly run with corrected weights for the zero-level reflections. The largest fractional coordinate change of this cycle was 4×10^{-4} . The refinement process was therefore terminated.

Final coordinates and temperature factors are shown in Table 8. The discrepancy factor based on these coordinates is 14.2 when reflections with $F_0 = 0$ are included in the computation and 11.5 when these are omitted.

Chapter VII

Final structure

The structure of narsarsukite is illustrated in Figs. 8 and 9. Narsarsukite has a new type of silica tetrahedra arrangement whose silicon to oxygen ratio is 4:10. The formula should be written $\text{Na}_2\text{TiOSi}_4\text{O}_{10}$ since some oxygen atoms are coordinated only by titanium and sodium atoms. Fig. 8 is a projection of the structure from $z = 0$ to $z = \frac{1}{2}$ on (xyO) . Fig. 9a is a three-dimensional representation of a section of the new silica tetrahedra arrangement, while Fig. 9b is a simplified drawing of this same type of arrangement.

The main points involved in an understanding of the structure of narsarsukite may be appreciated with reference to Fig. 8. A crystal may be built from this unit by repetitions involving translations uvO and reflections across mirrors at $z = 0$ and $z = \frac{1}{2}$, which are the limits of the portion of the crystal projected. There are two basic units in the structure. First, there is a series of titanium octahedra arranged along the four-fold axes. Each titanium atom shares an oxygen atom with the titanium atoms immediately above and below. There is thus an infinite chain of octahedra which share corners, the four-fold axis being the axis of the chain.

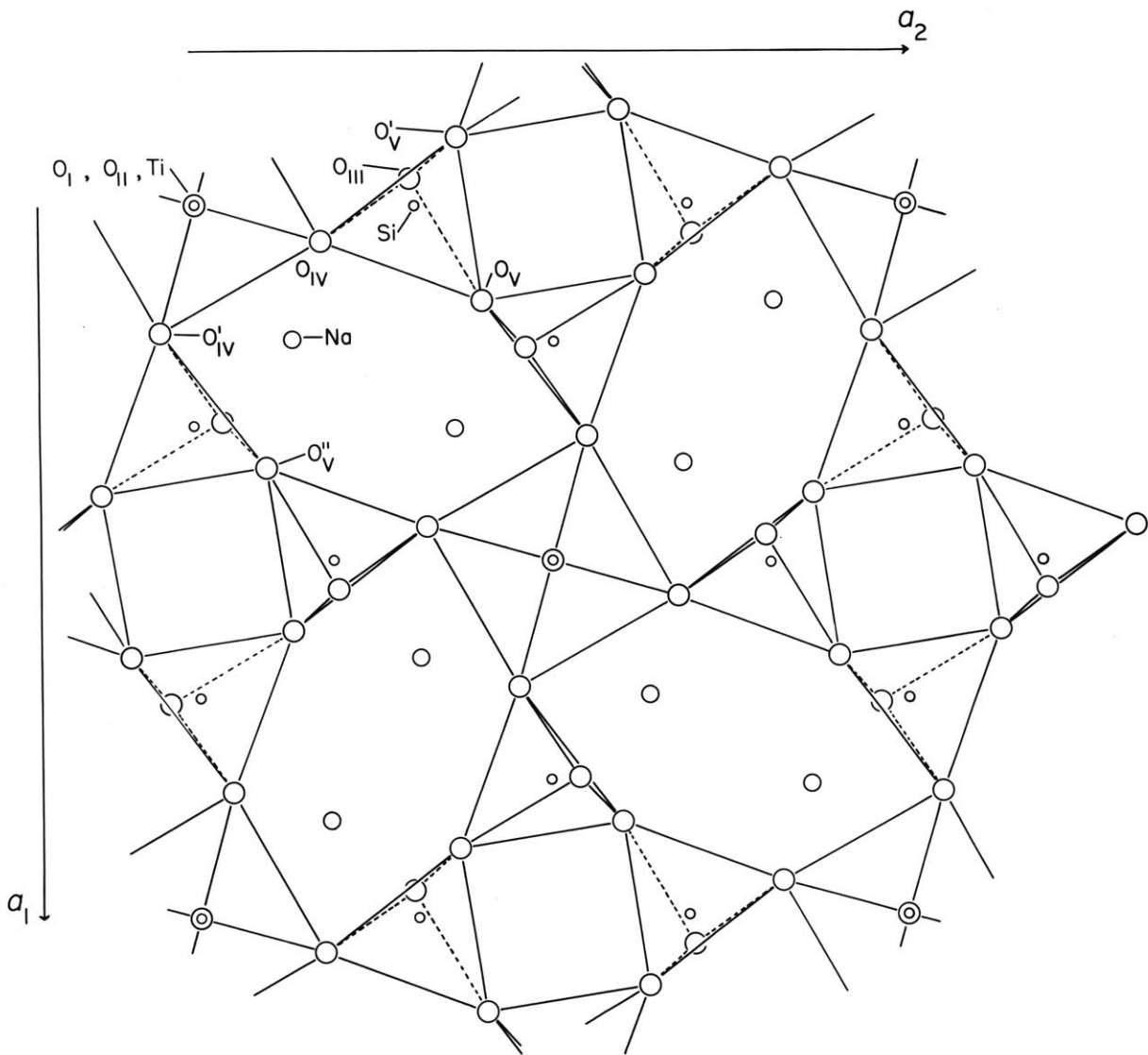


Fig. 8.

Projection of the structure from
 $z = 0$ to $z = \frac{1}{2}$ on $(xy0)$

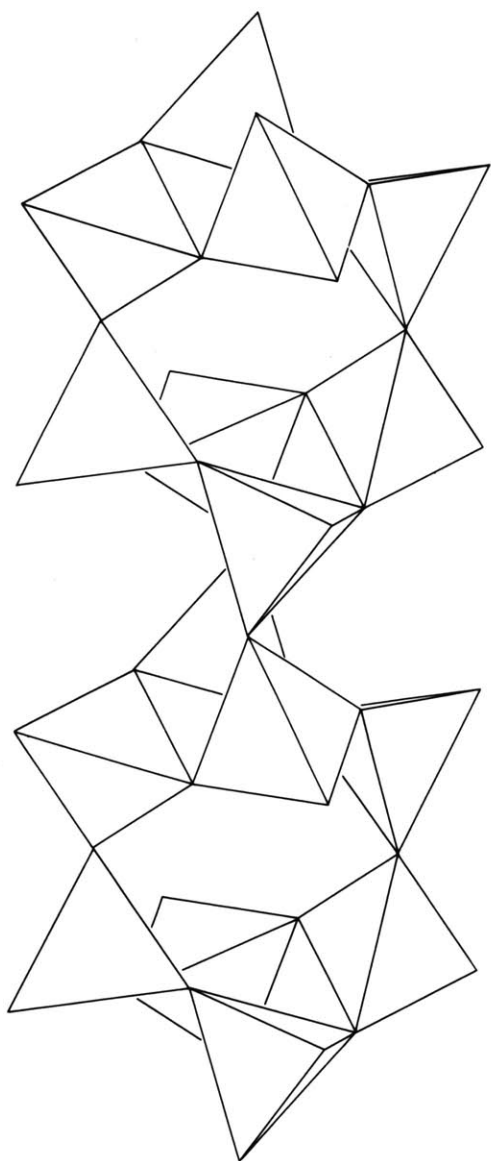


Fig. 9a

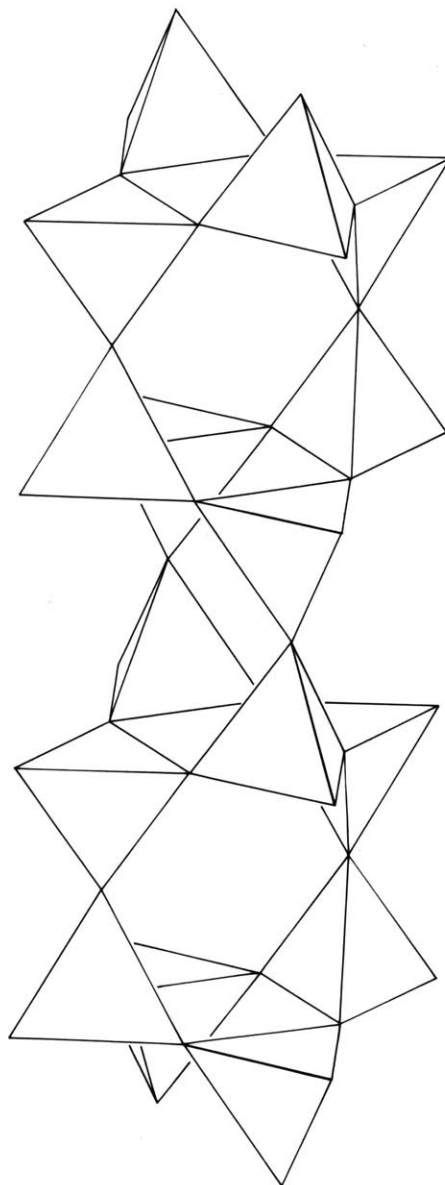


Fig. 9b

Fig. 9a. Tube of silica tetrahedra found in narsarsukite

Fig. 9b. Simplified version of the tube of silica tetrahedra found in narsarsukite

The second major unit of the structure is the network of silica tetrahedra. The tetrahedra are arranged around the $\bar{4}$ axes in rings of four, each tetrahedron sharing a corner with two other tetrahedra of the ring. They are oriented so that alternating tetrahedra of the ring point up and down. Thus two tetrahedra of each four-ring have vertices pointing up and two down. These vertices are shared by similar four-rings above and below. This arrangement can be appreciated by noting that the oxygen atoms shared by adjacent four-rings lie in mirror planes arranged parallel to the plane of the four-rings. The repetition of these four-rings in the c direction by the mirror planes yields a tube of tetrahedra arranged around the $\bar{4}$ axis.

The specific nature of the new silica tetrahedra arrangement can be readily grasped with reference to the simplified illustration of Fig. 9b. The four-rings of tetrahedra with vertices alternating up and down, bonded to four-rings above and below, are easily distinguished. This structure may be derived from the mica sheet network, which is a planar arrangement of six-rings. Let a narrow band, infinitely long, and two six-ring units wide, be separated from a mica sheet, as shown in Fig. 10. If this band is bent around parallel to its long axis, so that the long edges are bonded

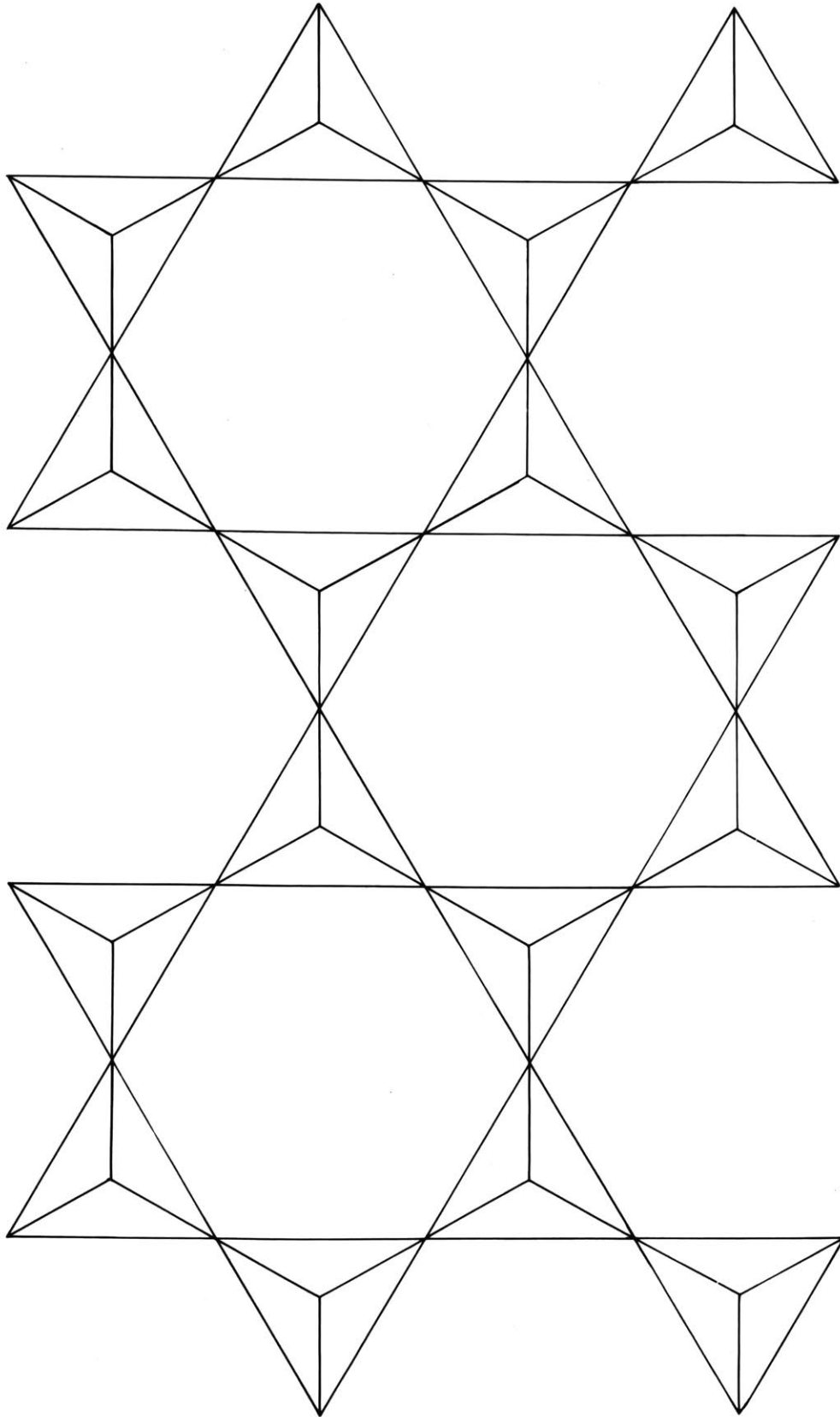


Fig. 10. Band of silica tetrahedra derived from a mica sheet

together, the silica tetrahedra tube of narsarsukite is obtained. The tetrahedra of the mica network which are arranged with unshared vertices pointing upward in Fig. 10 have unshared vertices pointing away from the axis of the tube. Thus each tetrahedron of the narsarsukite arrangement shares three vertices with other tetrahedra, as in the phyllosilicates.

Each tetrahedron has one corner unshared by other tetrahedra. It is the oxygen at this vertex which is bonded to a titanium atom, thus forming a bond between the chain of titanium octahedra and the tube of silica tetrahedra, both of which extend indefinitely in the c direction. The sodium atoms occupy the large voids between the chain of titanium octahedra and the tube of silica tetrahedra.

Interatomic distances are tabulated in Table 9. All four Si-O distances are approximately equal, suggesting that the oxygen arrangement around silicon approximates that of a tetrahedron. There are two Si-O-Si bond angles which are not symmetry equivalent. These involve adjacent tetrahedra of a four-ring, and adjacent tetrahedra of different four-rings. The Si-O-Si bond angles are 141.0° and 138.9° respectively. This compares fairly well with angles of 150° found by Nieuwenkamp in low quartz.^{3a}

Ti-O distances are relatively irregular, indicating

Table 9
Interatomic distances

Metal atom and coordinates	Number and type of oxygen neighbors and coordinates	Interatomic distance
Si x,y,z	1 O _{III} x,y,z	1.61 Å
	1 O _{IV} x,y,z	1.58
	1 O _V x,y,z	1.65
	1 O _V ⁱ $y-\frac{1}{2}, \frac{1}{2}-x, \frac{1}{2}-z$	1.62
Ti x,y,z	1 O _I x,y,z	1.90
	1 O _{II} x,y,z	2.08
	4 O _{IV} x,y,z	1.99
Na x,y,z	1 O _{II} x,y,z	2.48
	2 O _{IV} x,y,z	2.39
	2 O _{IV} ⁱ y, \bar{x}, z	2.72
	2 O _V ⁿ $\frac{1}{2}-x, \frac{1}{2}-y, \frac{1}{2}-z$	2.51

a moderate distortion of the octahedral arrangement of oxygen around titanium. The distortion involves the two oxygen atoms above and below the titanium atom on the four-fold axis. The titanium atom is closer to O_I (Ti-O = 1.90 Å) than to O_{II} (Ti-O = 2.08 Å). In addition, the z coordinate of the remaining four oxygen atoms of the titanium octahedron (.268) is greater than that of the titanium atom (.239). These oxygen atoms thus lie in a plane (normal to the four-fold axis) which is displaced away from the titanium atom toward O_{II} . In an ideal octahedron this plane includes the titanium atom. The titanium atom is thus displaced away from the center of the octahedron, toward one end. This effect is slightly accentuated by displacement of the four oxygen atoms (not on the four-fold axis) in the opposite direction. Exactly this same type of arrangement occurs^{4a} in tetragonal $BaTiO_3$. In this structure, titanium octahedra are bonded in a chain on the four-fold axes. The titanium atom is displaced 0.13 Å toward one end of the octahedron. Ti-O distances closely correspond to those of narsarsukite, as shown by the following table:

	narsarsukite	$BaTiO_3$
Ti-O // c	1.90 Å	1.869 Å
	2.08	2.107
Ti-O ⊥ c	1.99	1.999

The displacement of all titanium atoms toward the same end of the crystal is associated with ferroelectricity in BaTiO_3 . This property may be exhibited by $\text{Na}_2\text{TiOSi}_4\text{O}_{11}$ if an appropriate phase change from narsarsukite occurs.

Reference to Table 9 shows that seven oxygen atoms have Na-O distances which compare well with Na-O distances found in other crystal structures. Two of these oxygen atoms (O_V) have bonds which are probably saturated by silicon. If these two atoms are disregarded, the oxygen coordination around sodium is five. Reference to Fig. 8 shows that the polyhedron formed by these five oxygen atoms is very irregular. It does not actually enclose the sodium atom since all five oxygen atoms lie to one side of the sodium atom. This is also true, but to a lesser degree, even when the additional two oxygen atoms are included in the polyhedron.

Conformity of narsarsukite to Pauling's rules.

If the possibility of coordination of O_V with oxygen is excluded, O_V and O_{III} have electrostatic valency bonds exactly satisfied, since each is coordinated by two silicon atoms. Assuming a coordination of five oxygen atoms around sodium, the bonds from sodium to oxygen have electrostatic valency strengths of $1/5$. Titanium and silicon have electrostatic valency strengths of $4/6$ and 1 respectively. O_I and O_{II} are each coordinated by two titanium atoms, and four sodium atoms.

Their charge (-2) is slightly oversatisfied

$[2(4/6) + 4(1/5)] = 32/15$. O_{IV} is coordinated by one titanium atom, one silicon atom, and two sodium atoms.

Its charge is also slightly oversatisfied

$[1 + 4/6 + 2(1/5)] = 62/30$. If a coordination of six is assigned to sodium the electrostatic bonds are exactly satisfied. The extremely irregular coordination of oxygen around sodium, and the possibility that O_V should be included in the oxygen coordination sphere, makes exact calculation of electrostatic valencies complicated. The above calculations show that all bonds are satisfied within limits of interpretation of the sodium coordination.

Several points indicate that coordination may be much more complex than indicated above. It is possible that the two oxygen atoms (O_V) excluded above should be included in the sodium coordination sphere, especially since the two oxygen atoms (O_{IV}) with considerably larger Na-O distances were included. That these two oxygen atoms (O_V) are probably making some contribution to Na is shown by the relatively large Si- O_V distance (1.65 Å) which indicates that the oxygen atom may not be as closely bonded to silicon as usual. As noted above, inclusion of these two oxygen atoms in the sodium coordination polyhedron would make the polyhedron more regular.

If O_V is contributing some bond strength to sodium,

this oxygen atom cannot contribute its total bond strength to silicon. The resulting excess of silicon bond strength may be compensated for by O_{IV} . This oxygen atom exhibits an Si-O distance (1.58 Å) which is smaller than usual, indicating that it may be contributing more than a bond strength of -1 to silicon. In addition, this oxygen atom also has a very high Na-O distance, indicating that it may contribute little of its total bond strength to sodium. The "average" effect of O_{IV} and O_V may be such as to yield a six-fold oxygen coordination of sodium and a four-fold coordination of silicon, thus exactly satisfying Pauling's rule.

Bibliography

1. Gossner, B., and Strunz, H. (1932), Die chemische Zusammensetzung von Narsarsukit: Zeits. Krist., 82, 150-151.
2. Warren, B. E., and Amberg, C. R. (1934), X-ray study of narsarsukite, $\text{Na}_2(\text{Ti,Fe})\text{Si}_4\text{O}_{11}$: Am. Mineral., 19, 546-548.
3. Graham, William A. P. (1935), An occurrence of narsarsukite in Montana: Am. Mineral., 20, 598-601.
- 3a. Nieuwenkamp, W. (1935), Die Kristallstruktur des Tief-Cristobalits SiO_2 : Zeit. Krist., 92, 82-88.
4. Evans, R. G. (1952), Crystal Chemistry, Cambridge, Cambridge University Press.
- 4a. Megaw, Helen D. (1957), Ferroelectricity in Crystals, London, Methuen and Co.
5. Buerger, M. J., and Niizeki, N. (1958), Correction for absorption for rod-shaped single crystals: Am. Mineral., 43, 726-731.
6. Buerger, Martin J. (1959), Vector Space, New York, John Wiley and Sons.
7. Busing, R. William, and Levy, Henri A. (1959), A crystallographic least squares refinement program for the I. B. M. 704, Oak Ridge Tennessee, Oak Ridge National Laboratory.

8. Sly, William G., and Shoemaker, David P. (1959),
MIFRI: two-and three-dimensional crystallographic
Fourier summation program for the I. B. M. 704,
Mass. Insti. Tech..
9. Stewart, D. B. (1959), Narsarsukite from Sage
Creek, Sweetgrass Hills, Montana: Am. Mineral.,
44, 265-273.